Supporting Information for

A dramatic platform for oxygen reduction reaction based on silver nanoclusters

Xuan Yang, Linfeng Gan, Chengzhou Zhu, Baohua Lou, Lei Han, Jin Wang* and Erkang Wang*

State Key Laboratory of Electroanalytical Chemistry, Changchun Institute of Applied Chemistry, Chinese Academy of Sciences, Changchun, Jilin,130022, China, Graduate School of the Chinese Academy of Sciences, Beijing, 100039, China, College of Physics, Jilin University, Changchun, Jilin, P. R. China 130012 and Department of Chemistry and Physics, State University of New York at Stony Brook, New York 11794-3400.

*To whom correspondence should be addressed. E-mail: jin.wang.1@stonybrook.edu; ekwang@ciac.jl.cn

Experimental Section

Chemicals and materials. Sodium borohydride (98%) was obtained from Sigma-Aldrich Co. (USA). Commercial Pt/C catalyst was purchased from Aldrich (USA). All the other chemicals were of analytical reagent grade and were used as received without further purification. All the solutions were prepared with double-distilled water purified by a Milli-Q system (Millipore, Bedford, MA, USA).

Synthesis of Ag NCs. In a typical experiment, 34.0 mg $AgNO_3$ was dissolved in 20 mL ethanol. [1, 2] The solution was cooled to 0 °C in an ice bath; the ligand 2-mercaptobenzothiazole was then added respectively. The solution was slowly stirred for 4 h in an ice bath. After the complete formation of $Ag_x(MB)_y$ aggregated, $NaBH_4$ (7.6 mg, powders) was added to the solution under vigorous stirring. The reaction mixture slowly turned to deep brown, indicating the reduction of $Ag_x(MB)_y$ by $NaBH_4$ and the formation of Ag NCs. The reaction was allowed to proceed for 12 h under constant stirring at 0 °C. A brown suspension was finally obtained. The products were centrifuged at 13000 rpm for 10 min, the supernatants were removed and the resultant precipitates were collected and dissolved in ethanol again. Recrystallization for 3 times led to highly pure Ag NCs. The as-prepared clusters were dried under reduced pressure and finally dissolved in choloform for further use. The yield of Ag NCs was about 70% (Ag atom basis).

Synthesis of Ag NPs. In a typical synthesis of citrate protected Ag NPs with the diameter of 50-60 nm, [3] 0.125 mL of 0.2 M $AgNO_3$ aqueous solution was rapidly added into 50 mL water under vigorous stir. After heating to boil, 3 ml of 1% citrate aqueous solution was quickly added to the above solution, and followed by adding 0.1 M ascorbic acid (2 mL). A quick color change was observed upon the addition of ascorbic acid. After heating for 5 min, the solution was stored at ambient condition for characterization. MB protected Ag nanoparticles were synthesized by maintaining the Ag NCs protected by MB in chloroform at 30 °C for 60 days. After reacting for 60 days at 30 °C, the Ag NCs protected by MB were aggregated to form Ag NPs.

Characterizations. UV-visible absorbance spectra were recorded on a Cary 50 scan UV-vis-NIR spectrophotometer (Varian, Harbor City, CA) at room temperature. Photoluminescence spectra were carried out on a LS-55 luminescence spectrometer (Perkin-Elmer, USA). Fourier transform infrared spectra (FTIR) were measured on a Bruker IFS 66V/S Fourier transform infrared spectroscope (Germany). Mass spectra were carried out on Bruker autoflex III smartbeam matrix-assisted laser desorption/ionization time of flight/time of flight mass spectrometer (MALDI-TOF/TOF-MS) (Germany), the laser system was smartbeam laser with 355 nm wavelength and the scan mode was reflective/linear, the ion mode was positive under an acceleration voltage of 20.00 kV, the ion extraction time was 0 ns, the solvent was chloroform and the matrix was dithranol. Transmission electron microscopy (TEM) measurements were made on a FEI TECNAI G2 transmission electron microscope (Netherlands) operated at an accelerating voltage of 120 kV. X-ray diffraction (XRD) measurements

were made on a PW1700 X-ray diffractometer. X-ray photoelectron spectroscopy (XPS) measurements were made on a Thermo ESCALAB 250 X-ray photoelectron spectrometer. Atomic force microscopy was measured on a MultiMode® 8 Scanning Probe Microscope (Veeco Instruments Inc., USA) at room temperature, analyzed with NanoScope® Version 8.1 software. Nitrogen adsorption isotherm was recorded on an AUTOSORB-1 automated surface area and pore size analyzer (Quantachrome Instruments Inc., USA).

Electrochemical measurements. Electrochemical measurements for ORR were performed using a typical three-electrode electrochemical cell. Ag/AgCl and Pt were selected as reference electrode and the counter electrode, respectively. The glassy carbon electrode acted as working electrode. The commercial Pt/C were dispersed in deionized water + isopropanol + 5% Nafion (v/v/v = 4/1/0.05) to reach a concentration of 2 mg/mL. 10 μL of these dispersions were deposited on the surface of the glassy carbon electrode and dried under ambient conditions. Ag nanoclusters and different agents protected Ag nanoparticles were well dispersed in chloroform and deionized water at a concentration of 2 mg/mL, repectively. 10 mL of the solution were deposited on the surface of the glassy carbon electrode and dried under ambient conditions, and then 2.5 μL 0.2% Nafion was deposited on the surface of the glassy carbon electrode, followed by drying naturally. CV plots were collected in KOH solution (0.1 M) at a scanning rate of 100 mV s^{-1}. The polarization curves for ORR were conducted through the rotating disk electrode (RDE) technique with a scanning rate of 10 mV s^{-1}. The electrolyte was N_2 or O_2 saturated 0.1 M KOH.

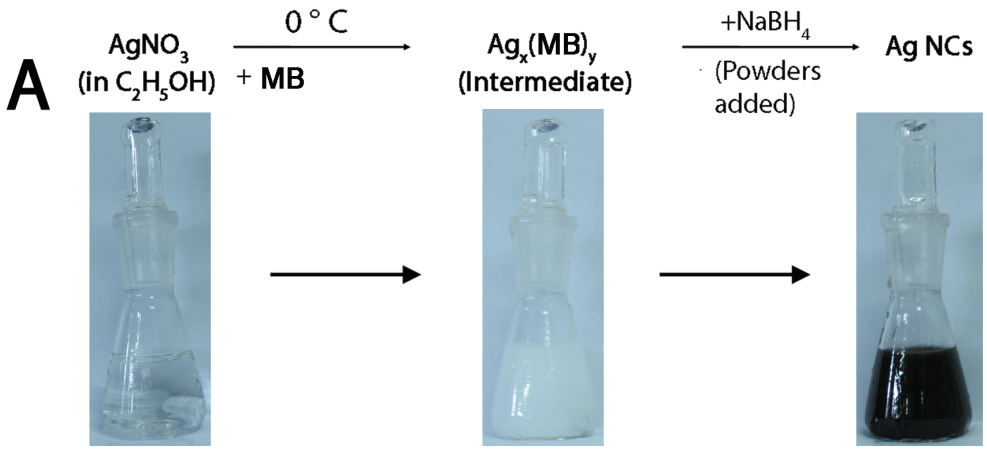

Supplementary Figure S1. The whole synthesis approach of Ag NCs protected by 2-mercaptobenzothiazole (MB). Ethanol solution of $AgNO_3$ (Left). 4 h after addition of MB (Middle). 12 h after addition of $NaBH_4$ (Right). The reaction was processed at 0 °C.

As shown in Supplementary Figure S1, silver nitrate was first dissolved in ethanol, and then the ligands were added. The solution was slowly stirred for 4 h in an ice bath. Then $NaBH_4$ was added to the solution under vigorous stirring. [1, 2] After the whole synthesis process of Ag NCs protected by MB, a brown suspension was finally obtained. The Ag NCs had a low solubility in the chosen reaction medium (ethanol) mainly because of that the scaffolds were not well soluble in ethanol, therefore, the resultant Ag NCs extracted from ethanol in a spontaneous depositing process. After reaction for 12 h, the products were centrifuged at 13000 rpm for 10 min, the supernatants were removed and the resultant precipitates were collected and dissolved in ethanol again. Recrystallization for 3 times led to highly pure MB protected Ag NCs. The as-prepared clusters were dried under reduced pressure, and finally the yield of Ag NCs was about 70% (Ag atom basis).

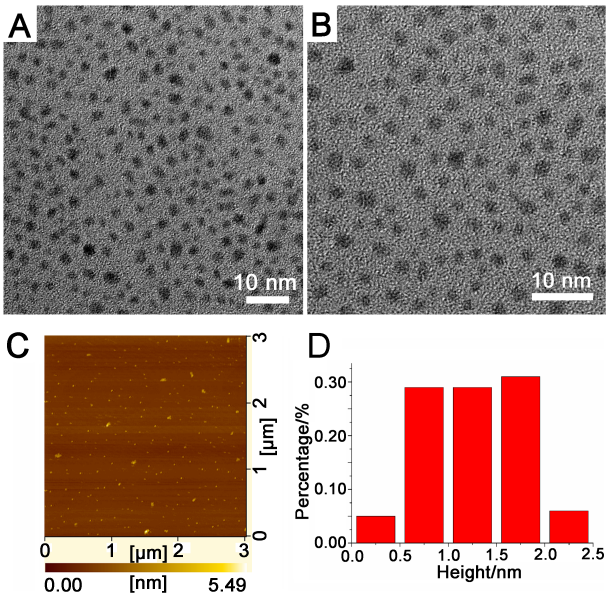

Supplementary Figure S2. Typical TEM images (A, B), AFM image (C) and the height distributions (D) of Ag NCs.

Transmission electron microscopy (TEM) and atomic force microscopy (AFM) were used to directly observe the size distributions of the Ag NCs protected by MB and thus characterize their nanostructures. The diameters of most Ag NCs ranged from 0.5 to 2.0 nm, which was consistent with the definition of nanoclusters (<2 nm). There might have been some smaller Ag NCs present, but because of the low resolution of the transmission electron microscope, these Ag NCs were not observed. There were some large nanoparticles with the diameters larger than 2 nm and these Ag NPs might be aggregations of small Ag NCs.

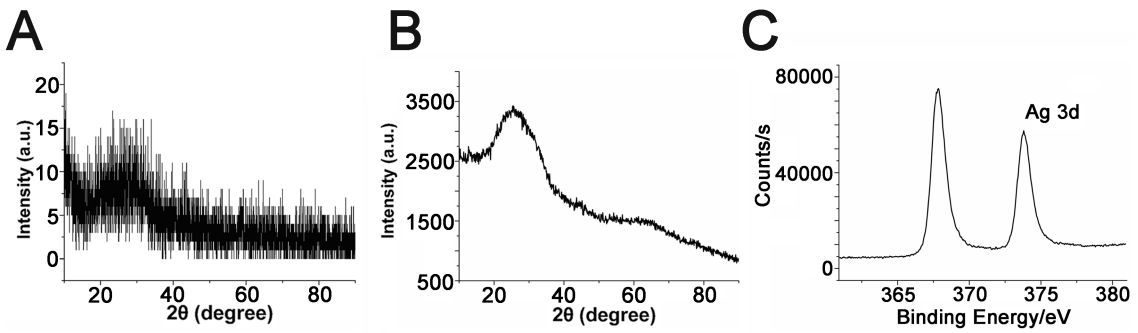

Supplementary Figure S3. The XRD patterns of blank (A) and the silver nanoclusters (B) and the XPS spectra of the silver nanoclusters (C).

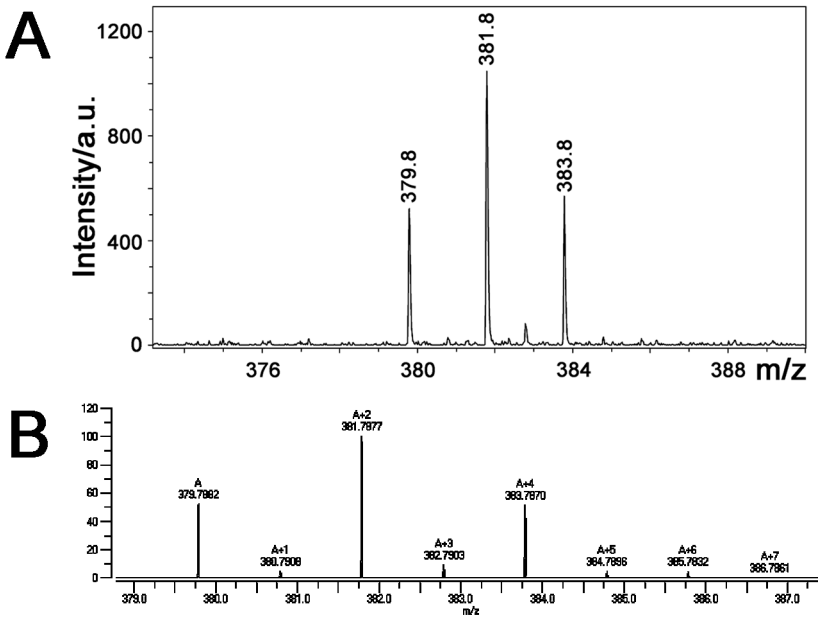

Supplementary Figure S4. The MALDI-TOF/TOF mass spectrum of $[Ag_2(MB)\text{-}H]^+$ (A) and the theoretical spectrum of $[Ag_2(MB)\text{-}H]^+$ (B).

Supplementary Figure S4 A showed the MALDI-TOF/TOF mass spectrum of $[Ag_2(MB)\text{-}H]^+$ and Supplementary Figure S4 B showed the theoretical spectrum of $[Ag_2(MB)\text{-}H]^+$ which was consistent with the experimental spectrum. [1]

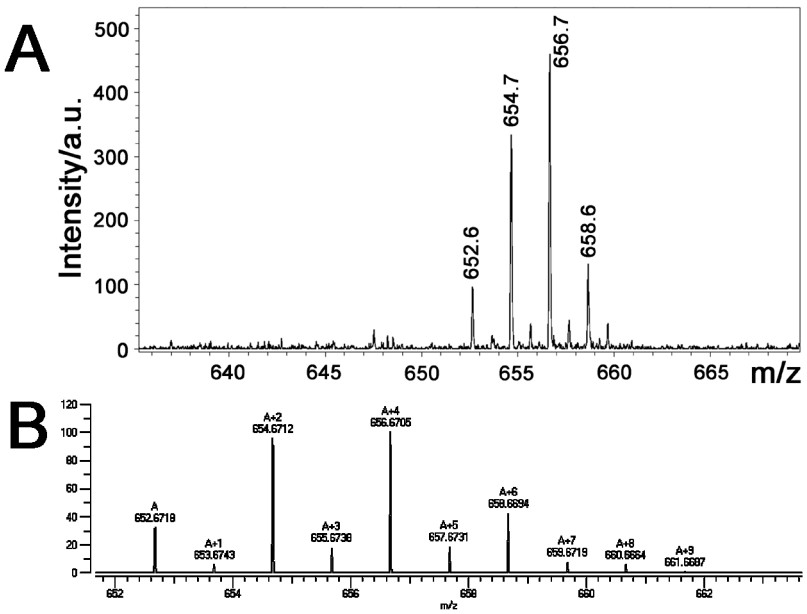

Supplementary Figure S5 The MALDI-TOF/TOF mass spectrum of $[Ag_3(MB)_2\text{-}2H]^+$ (A) and the theoretical spectrum of $[Ag_3(MB)_2\text{-}2H]^+$ (B).

Supplementary Figure S5 A showed the MALDI-TOF/TOF mass spectrum of $[Ag_3(MB)_2\text{-}2H]^+$ and

Supplementary Figure S5 B showed the theoretical spectrum of $[Ag_3(MB)_2\text{-}2H]^+$ which was consistent with the experimental spectrum. [1]

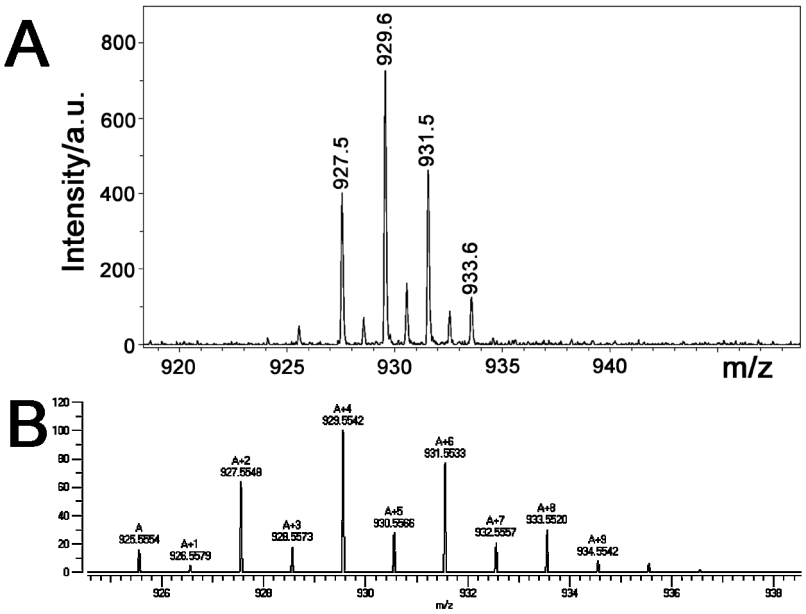

Supplementary Figure S6. The MALDI-TOF/TOF mass spectrum of $[Ag_4(MB)_3\text{-}3H]^+$ (A) and the theoretical spectrum of $[Ag_4(MB)_3\text{-}3H]^+$ (B).

Supplementary Figure S6 A showed the MALDI-TOF/TOF mass spectrum of $[Ag_4(MB)_3\text{-}3H]^+$ and Supplementary Figure S6 B showed the theoretical spectrum of $[Ag_4(MB)_3\text{-}3H]^+$ which was consistent with the experimental spectrum. [1]

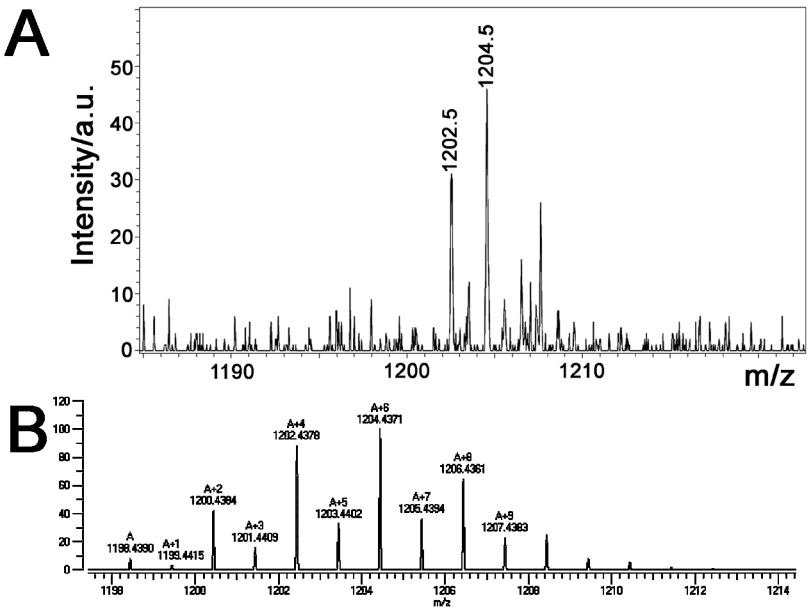

Supplementary Figure S7. The MALDI-TOF/TOF mass spectrum of $[Ag_5(MB)_4\text{-}4H]^+$ (A) and the theoretical spectrum of $[Ag_5(MB)_4\text{-}4H]^+$ (B).

Supplementary Figure S7 A showed the MALDI-TOF/TOF mass spectrum of $[Ag_5(MB)_4\text{-}4H]^+$ and Supplementary Figure S7 B showed the theoretical spectrum of $[Ag_5(MB)_4\text{-}4H]^+$ which was consistent with the experimental spectrum. [1]

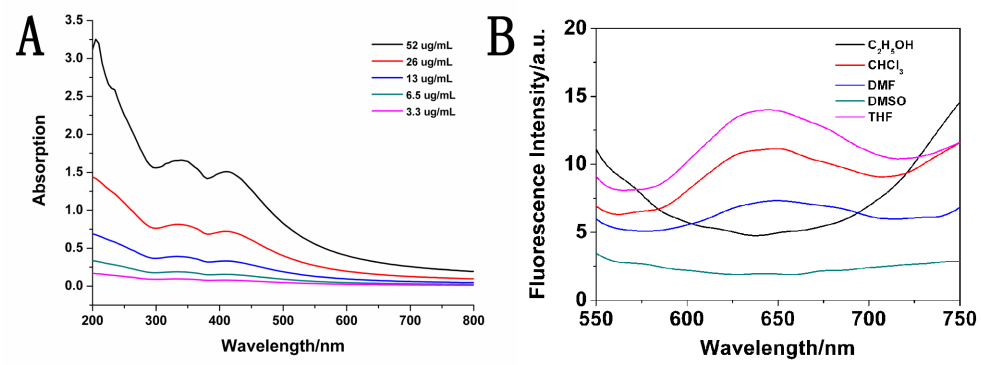

Supplementary Figure S8. The UV-visible absorption of different concentrations of MB protected Ag nanoclusters in chloroform (A) and fluorescence spetra of MB protected Ag nanoclusters in different solvents.

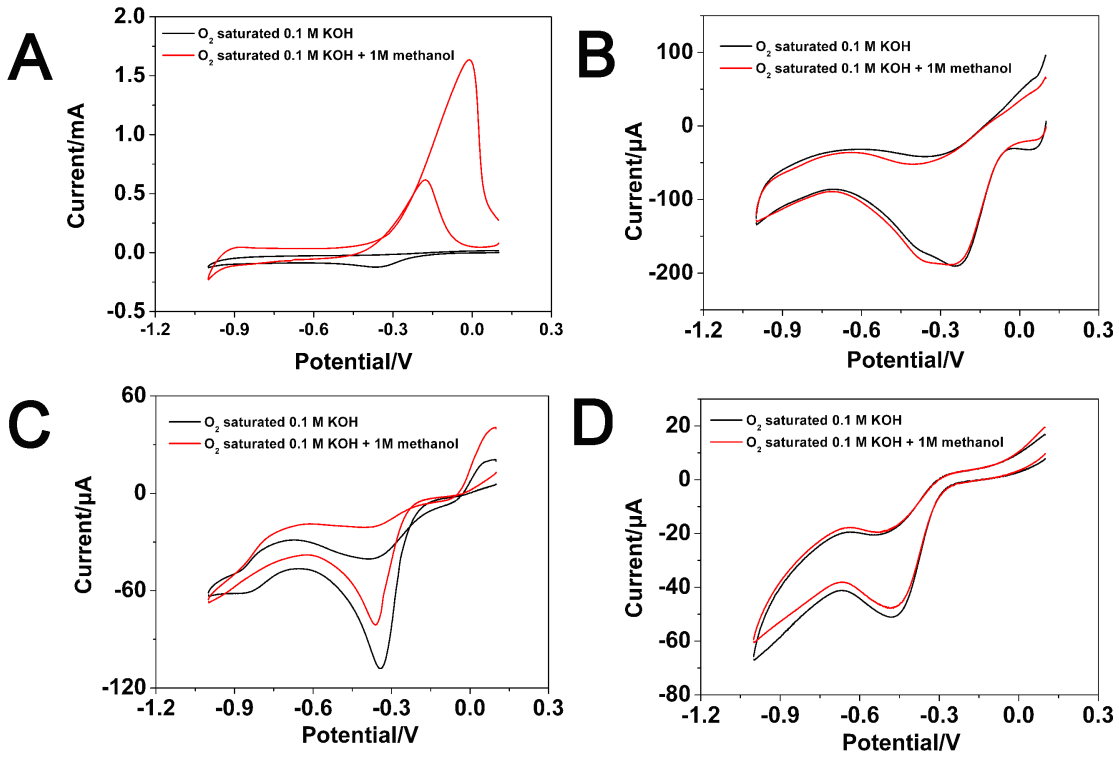

Supplementary Figure S9. CV curves of commercial Pt/C (A), Ag NCs (B), citrate protected Ag NPs (C) and MB protected Ag NPs (D) in O_2-saturated 0.1 M KOH solution with and without 1 M CH_3OH. Scan rate: 100 mV s^{-1}.

For further characterizations of the ORR activity of the Ag NCs, these catalysts were further compared by separately introducing O_2 and methanol into the electrolyte to examine their possible selectivity and crossover effects via CV measurements. (Supporting information, Figure S9) Addition of 1 M methanol to the O_2 saturated electrolyte did not affect the catalytic activity of the Ag NCs towards ORR. In contrast, a pair of peaks at ca. -0.17 and -0.013 V were observe for methanol oxidation on commercial Pt/C electrode, whereas the cathodic peak for ORR had vanished. There were no additional peaks for methanol oxidation observed on the Ag NPs protected by citrate and MB electrode. However, the peak currents of citrate and MB protected Ag NPs decreased about 25% and 8%, respectively.

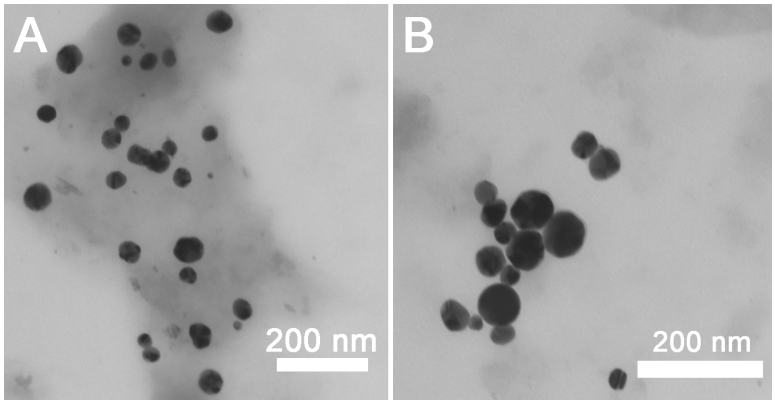

Supplementary Figure S10. Typical TEM images of citrate protected Ag NPs.

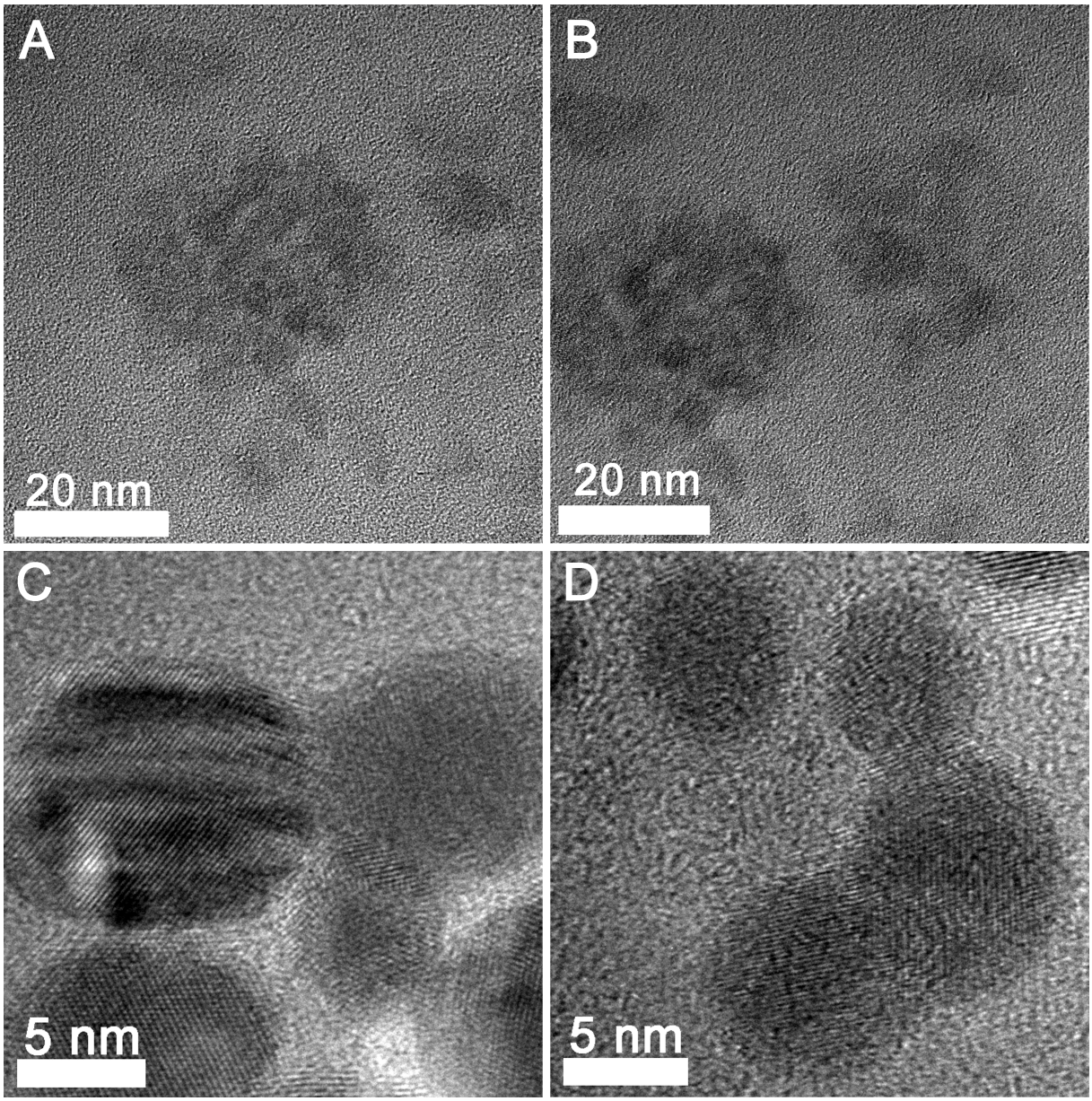

Supplementary Figure S11. Typical TEM images of MB protected Ag NPs.

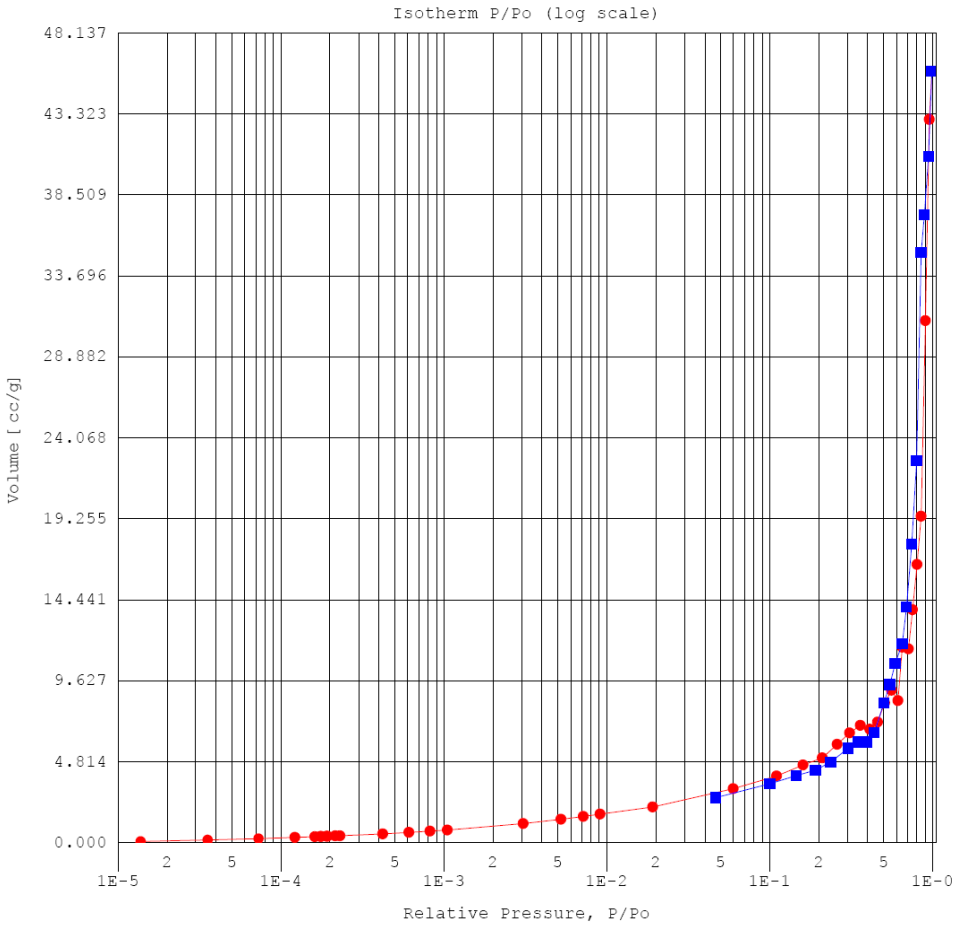

Supplementary Figure S12. Nitrogen adsorption isotherm for MB protected Ag NCs.

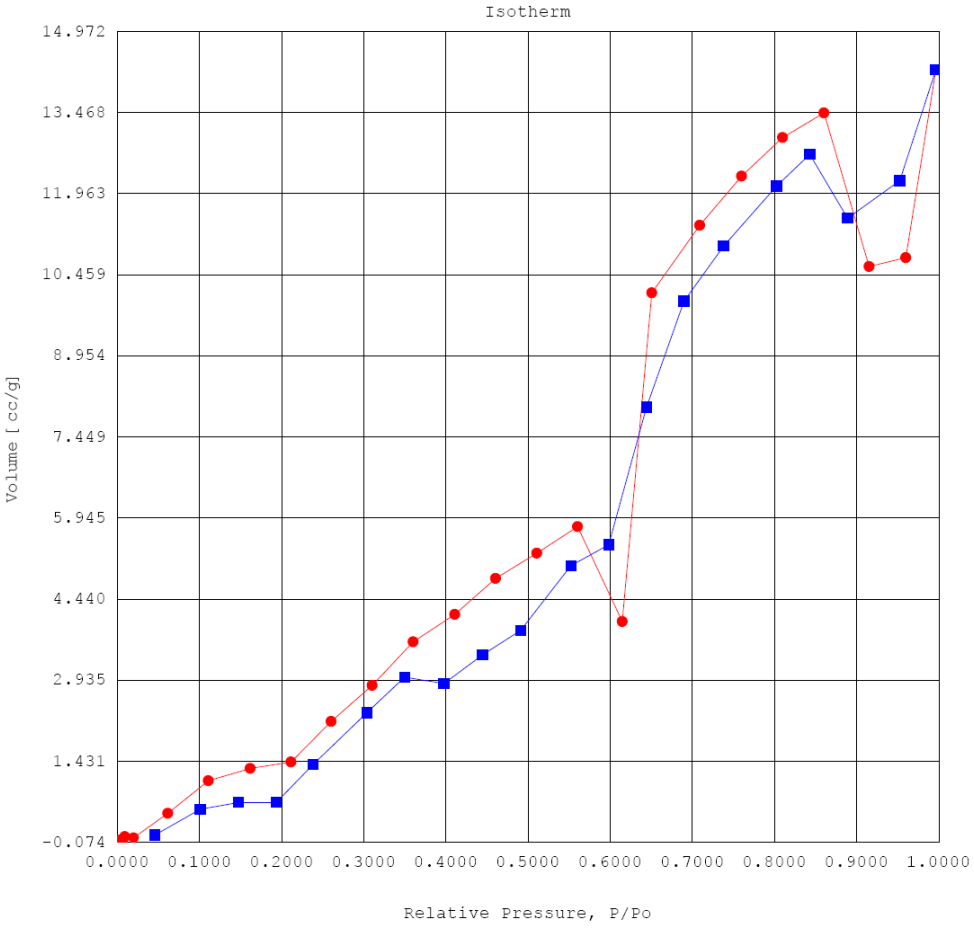

Supplementary Figure S13. Nitrogen adsorption isotherm for citrate protected Ag NPs.

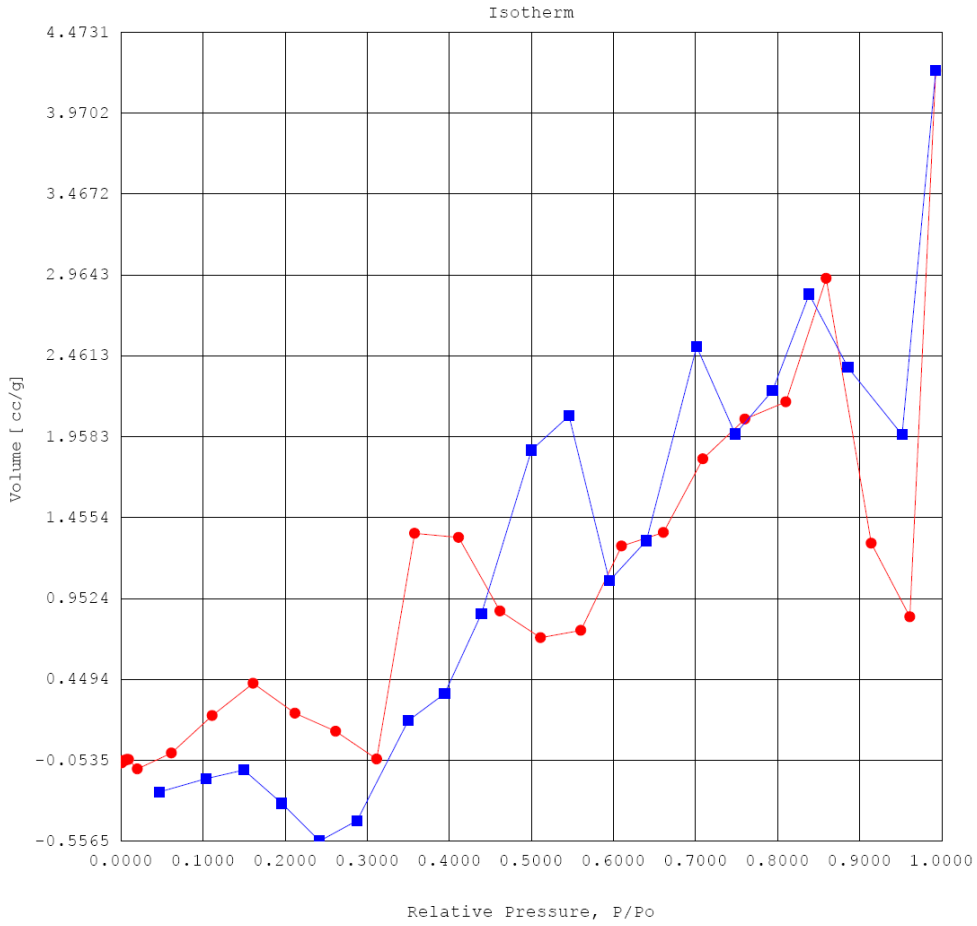

Supplementary Figure S14. Nitrogen adsorption isotherm for MB protected Ag NPs.

According to the nitrogen adsorption isotherm results of Ag NCs, citrate protected Ag NPs, and MB protected Ag NPs in Figure S12, S13 and S14, the specific surface area of Ag NCs was 21.17 m^2 g^{-1} and the specific surface area of Ag NPs protected by citrate and MB were too small that it could not be detected by the equipment.

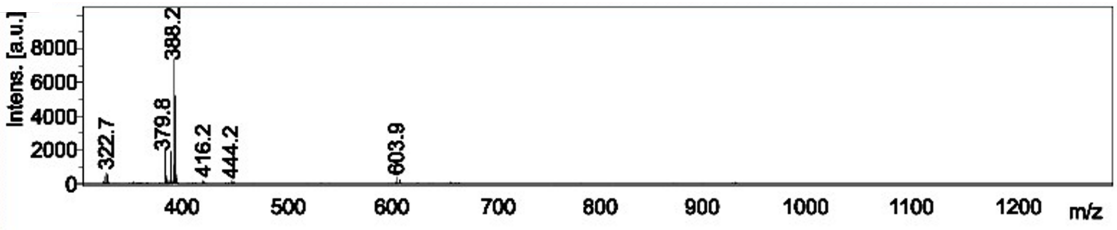

Supplementary Figure S15. MALDI-TOF/TOF mass spectra of intermediate.

electrocatalysts	E_{peak} (V) [a]	j_{peak} (mA cm^{-2}) [a]	E_{onset} (V) [b]	$E_{1/2}$ (V) [b]	j (mA cm^{-2}) at -0.6 V [b]
commercial Pt/C	-0.27	-0.52	-0.11	-0.28	-3.61
Ag NCs	-0.19	-0.67	-0.07	-0.20	-3.41
Citrate protected Ag NPs	-0.35	-0.77	-0.26	-0.33	-1.73
MB protected Ag NPS	-0.46	-0.26	-0.31	-0.38	-1.25

[a] Obtained from Figure 2A

[b] Obtained from Figure 2B

Table S1. Electrochemical parameters for ORR estimated from CVs and RDE polarization curves in 0.1 M KOH solution.

Reference:

1. Z. K. Wu, E. Lanni, W. Q. Chen, M. E. Bier, D. Ly, R. C. Jin, *J. Am. Chem. Soc.* **2009**, *131*, 16672-16674.
2. X. Yang, L. F. Gan, L. Han, E. K. Wang, J. Wang, *Angew. Chem. Int. Ed.* **2013**, *52*, 2022-2026.
3. S. J. Guo, S. J. Dong, E. K. Wang, *Chem. Eur. J.* **2008**, *14*, 4689-4695.